0026-895X/94/050899-09$03.00/0

MOLECULAR PHARMACOLOGY, 45:899-907

Characterization of [^{3}H]Ba 679 BR, a Slowly Dissociating Muscarinic Antagonist, in Human Lung: Radioligand Binding and Autoradiographic Mapping

EL-BDAOUI HADDAD, JUDITH C. W. MAK, and PETER J. BARNES

Department of Thoracic Medicine, National Heart and Lung Institute, London, SW3 6LY UK

Received September 16, 1993; Accepted February 21, 1994

SUMMARY

Ba 679 BR [7(*S*)-(1α,2β,4β,5α,7β)-7-[(hydroxydi(2-thienyl) acetyl)oxy]-9,9-dimethyl-3-oxa-9-azoniatricyclo[3.3.1.0^{2,4}]nonane bromide] is a new long-acting muscarinic antagonist developed as a bronchodilator drug. In this study, we have evaluated its affinity, its selectivity, and the distribution of its binding sites in human lung. [^{3}H]Ba 679 BR binds to a homogeneous population of muscarinic receptors in human lung membranes, with affinities in the subnanomolar concentration range. Like ipratropium bromide, Ba 679 BR showed no selectivity in its interactions with rat cerebrocortical M_1 receptors (labeled with [^{3}H]telenzepine) or heart M_2 and salivary gland M_3 receptors [labeled with [*N-methyl*-^{3}H]scopolamine ([^{3}H]NMS)]. Ba 679 BR displayed 6–20-fold higher affinity, compared with ipratropium bromide. We also studied the rate of Ba 679 BR and ipratropium bromide dissociation from human lung muscarinic receptors, by monitoring [^{3}H]NMS association. Unlike ipratropium bromide (100 nM), which dissociated so quickly that there was little difference in the [^{3}H]NMS association, compared with vehicle-treated membranes, Ba 679 BR (1 nM) had a strong protective effect against [^{3}H]NMS binding (>70%) that lasted for 90 min. Kinetic experiments conducted with [^{3}H]Ba 679 BR confirmed the slow dissociation profile of this compound. The dissociation rate constant (k_{-1}) for [^{3}H]Ba 679 BR was 3.29 ± 0.18 × 10^{-3} min^{-1}, corresponding to a half-life of the complex of 212 ± 11 min. Autoradiographic studies revealed that [^{3}H]Ba 679 BR binding sites were densely distributed in alveolar walls and submucosal glands. These results suggest that the slow dissociation profile of Ba 679 BR from human lung muscarinic receptors might be the underlying mechanism by which this drug achieves its long duration of action observed in functional tests.

Accumulating evidence suggests the classification of muscarinic receptors into four major subtypes (M_1-M_4) on the basis of their antagonist affinities (1–3). These receptors are differentially distributed, with a high density of M_1 receptors in cerebral cortex, M_2 receptors in heart, cerebellum, and smooth muscle, M_3 receptors in exocrine glands, and M_4 receptors in rabbit lung and bovine adrenal medulla. The molecular cloning of five muscarinic receptor genes (m1-m5) has provided the molecular basis of muscarinic receptor subtypes (4). Experiments on the expression of cloned receptors in mammalian cells proved the activity of these receptors and showed their specific coupling to different second messenger pathways and ionic currents. The tissue expression and the antagonist-binding properties of the m1-m4 gene products correlate well with the pharmacologically defined M_1-M_4 receptors (3, 5–7). Although mRNA for the m5 receptor has been located in restricted brain areas (8), there are no reports on pharmacological studies of this receptor in tissues.

In mammalian airways, the dominant neural bronchoconstrictor mechanism is provided by cholinergic nerves (9). Muscarinic receptor subtypes have been identified in airways of several species, including humans (10). Three muscarinic receptors have been identified in airways of humans and in several animal species. M_1 receptors are localized to parasympathetic ganglia (11) and to sympathetic nerve terminals, whereas M_2 receptors are localized in the postganglionic cholinergic nerves and provide functional negative feedback modulation of acetylcholine release (12). Excitatory M_3 receptors localized to airway smooth muscle and mucosal glands mediate bronchoconstriction (13) and mucus secretion (10). The occurrence of M_4 receptors has been demonstrated in rabbit lung but their role in airway function remains to be determined (14, 15). The presence of at least three muscarinic receptor subtypes in human airways raises the possibility of more selective anticholinergic therapy of airway obstruction in the future.

Muscarinic receptors play an important role in human airway smooth muscle contraction and submucosal gland secretion. Patients with asthma and chronic obstructive airway disease suffer from bronchoconstriction and enhanced mucus production, which can be relieved by cholinergic antagonists such as ipratropium bromide (16).

This work was supported by Boehringer Ingelheim (Ingelheim-am-Rhein, Germany). We thank the Medical Research Council (UK) for support.

ABBREVIATIONS: NMS, *N*-methylscopolamine; 4-DAMP, 4-diphenylacetoxy-*N*-methylpiperidine.

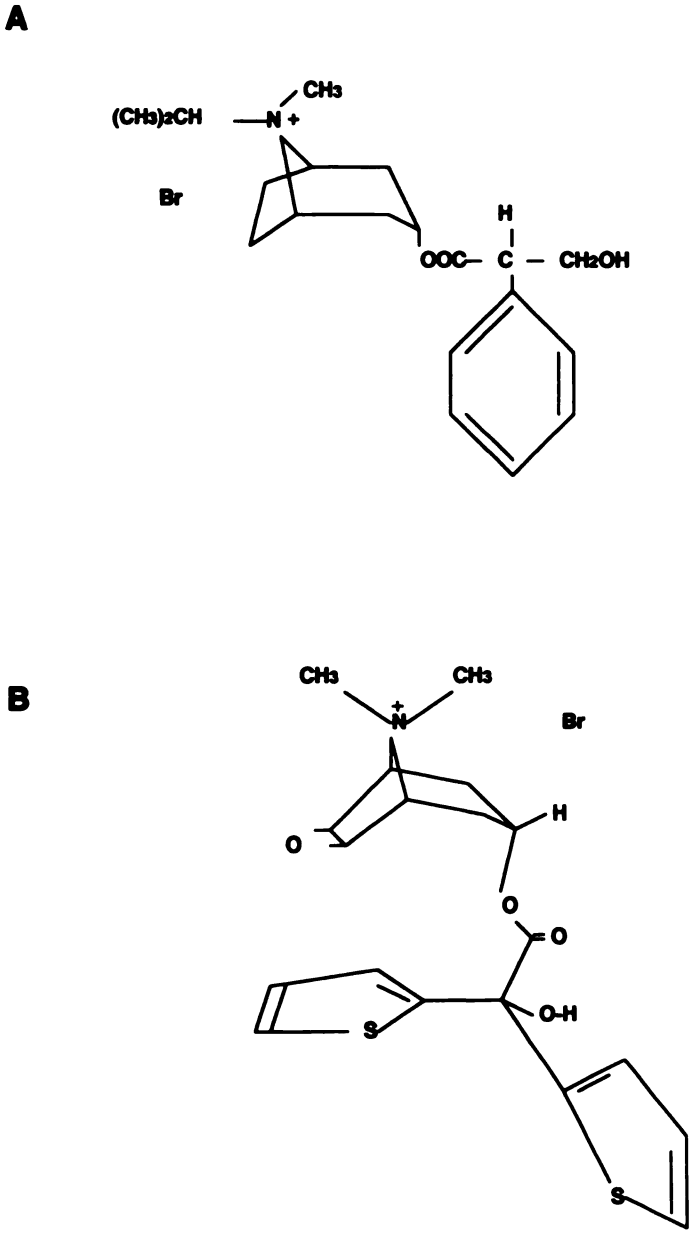

Fig. 1. Chemical structures of ipratropium bromide (A) and Ba 679 BR (B).

Recently, Ba 679 BR (Fig. 1) was introduced as a new bronchodilator drug with a long duration of action (17). In this study, we have investigated the binding characteristics of Ba 679 BR in human lung membranes. The pharmacological profile of Ba 679 BR was also determined in rat cerebral cortex using [^{3}H]telenzepine to label M_1 receptors and in rat heart and salivary glands using [^{3}H]NMS to label M_2 and M_3 receptors, respectively. The nonselective muscarinic antagonist ipratropium bromide was included in this study as a reference drug. We also studied the binding characteristics of [^{3}H]Ba 679 BR and used autoradiographic mapping to determine the tissue distribution of [^{3}H]Ba 679 BR binding sites in human lung and trachea.

Experimental Procedures

Materials. [^{3}H]NMS (79.5 Ci/mmol) was obtained from DuPont New England Nuclear (Boston, MA). [^{3}H]Ba 679 BR (80 Ci/mmol) was kindly provided by Boehringer Ingelheim (Ingelheim, Germany). Ipratropium bromide was obtained from Research Biochemical Inc. (Natick, MA), and atropine sulfate and pirenzepine dihydrochloride were from Sigma Chemical Co. (St. Louis, MO). The following compounds were gifts: Ba 679 BR [7(S)-(1α,2β,4β,5α,7β)-7-[(hydroxydi(2-thienyl)acetyl)oxy]-9,9-dimethyl-3-oxa-9-azoniatricyclo[3.3.1.0^{2,4}]nonane bromide] (Boehringer Ingelheim, Germany), methoctramine (C. Melchiorre, Bologna, Italy), and 4-DAMP (R. B. Barlow, Bristol, UK).

Membrane preparations. Human lungs were obtained from 21 heart-lung transplant donor patients (age, 22 ± 8 years; nine men) with brain death, in whom there was no evidence of heart or lung disease. Lung tissue was immediately placed into oxygenated Krebs-Henseleit solution (118 mM NaCl, 5.9 mM KCl, 1.2 mM $MgSO_4$, 2.5 mM $CaCl_2$, 1.2 mM NaH_2PO_4, 25.5 mM $NaHCO_3$, 5.6 mM glucose; cooled to 4°) and was transported to the laboratory. The peripheral lungs were dissected in physiological solution, frozen in liquid nitrogen, and stored at −80° before preparation of membranes. Cerebral cortex, heart, and salivary glands were obtained from male Wistar rats.

All membrane preparation procedures were performed at 4°. Human lung and rat heart, cerebral cortex, and salivary glands were finely minced with scissors and homogenized in 10–20 volumes (w/v) of ice-cold 0.35 M sucrose, 25 mM Tris·HCl, with an Ultra-Turax homogenizer (10–15 bursts). After centrifugation at 800 × g for 10 min at 4°, the pellets were suspended, homogenized, and resedimented at the same speed. The supernatants from these two stages were pooled and diluted with 50 volumes of ice-cold 25 mM Tris buffer, pH 7.4. The membranes were pelleted by centrifugation at 40,000 × g for 20 min. The resulting pellets were resuspended in an appropriate volume of buffer. For human lung, membranes were washed two additional times. The membrane suspension was then stored as aliquots at −80°. The protein concentration was determined according to the method of Lowry *et al.* (18).

Binding assays. All binding studies were performed in 1 ml of 25 mM Tris buffer, pH 7.4, containing the following tissue concentrations: cerebral cortex, 100–200; heart, 200–400; salivary glands, 100–200; and human lung, 300–600 μg of protein/ml. In competition experiments using [^{3}H]NMS or [^{3}H]Ba 679 BR a fixed concentration of 0.6 nM was used, whereas in studies involving [^{3}H]telenzepine a final radioligand concentration of 0.4 nM was used. ^{3}H-labeled antagonist saturation curves were obtained using concentrations ranging from 0.04 to 8 nM. Incubations were performed at 30° for 2.5–3 hr and were terminated by rapid vacuum filtration over 0.2% polyethyleneimine-pretreated glass fiber filters, using a Brandel cell harvester. The filters were washed twice with 4 ml of ice-cold Tris buffer, placed in vials with 4 ml of scintillation cocktail (Filtron X; National Diagnostics, Manville, NJ), and counted in a liquid scintillation counter (model 2200 CA; Packard, Meriden, CT). Due to the extremely slow dissociation kinetics of [^{3}H]Ba 679 BR in human lung, control competition experiments using this radioligand were also examined after a 24-hr incubation period, to ensure that full equilibrium was reached under our conditions (see Results).

Kinetic studies. To investigate the reversibility of muscarinic antagonist binding, aliquots of human lung membranes were treated for 3 hr at 30° with assay buffer (control), Ba 679 BR (1 nM), or ipratropium bromide (100 nM). After this preincubation period, membranes were diluted (1/70) with buffer containing [^{3}H]NMS (final concentration, 0.5 nM), to induce dissociation of antagonist. [^{3}H]NMS binding was measured at various time intervals. The concentrations of antagonists used in this set of experiments were calculated to occupy 80–90% of receptors. Nonspecific binding was defined as binding in the presence of 1 μM atropine. Specific [^{3}H]NMS binding in the presence of antagonists was corrected for protein concentration and expressed as a percentage of the value obtained for binding to control membranes.

In kinetic experiments involving [^{3}H]Ba 679 BR, human lung membranes were incubated with 0.63 nM [^{3}H]Ba 679 BR in the absence or presence of 1 μM atropine. [^{3}H]Ba 679 BR dissociation was determined, after equilibrium had been reached, by dilution with 10 μM atropine, and specific binding was determined at appropriate time intervals.

Data analysis. Data for the saturation and inhibition studies were analyzed using the nonlinear regression analysis described by Munson and Rodbard (19). The precision of fit to a one- or two-site model was determinated with an F test ($p < 0.01$), by comparing the residual sum of squares for fitting data to a one- or two-site model. Kinetic experiments were analyzed as described previously (20). Data are expressed as means ± standard errors.

Receptor autoradiography. Fresh and macroscopically normal human lungs and airways (segmental bronchus and trachea) were dissected. Lungs were inflated with tissue-embedding medium (OCT compound; Tissue-Tek, Naperville, IL) diluted 1/4 with phosphate-buffered saline, pH 7.4. Tissues were rapidly frozen in dichlorodifluoromethane (Arcton 12; ICI Research Laboratories, Runcorn, UK) cooled by liquid nitrogen. Serial cryostat sections of 10–16 μm were thaw-mounted on gelatin-coated microscope slides and stored at −80° until use.

To characterize [³H]Ba 679 BR binding to human lung sections, slides bearing three sections (16-μm thick) were washed for 5 min in incubation buffer (25 mM Tris·HCl, 0.25% Polypep, pH 7.4) at 30° and incubated for 3 hr in the presence of increasing concentrations of [³H]Ba 679 BR (0.08–8 nM). Nonspecific binding was determined by incubating alternate serial sections in the presence of 1 μM atropine. After incubation, slides were washed twice in Tris·HCl buffer at 4° for 15 min to remove unbound radioligand. Sections were then scraped from slides into scintillation vials, using Whatman GF/C filters; 4 ml of scintillant were added, and the radioactivity was quantified in a liquid scintillation counter. Several parallel sections were collected for protein determination. All incubations were performed in triplicate.

For autoradiographic studies, sections (10-μm thick) were warmed to room temperature and washed in 25 mM Tris·HCl, 0.25% Polypep, for 5 min. Slides were then incubated for 2.5 hr at 30° in Coplin jars with 25 ml of assay buffer containing a final [³H]Ba 679 BR concentration of 0.6 nM, with or without selective muscarinic antagonists. Nonspecific binding was determined by parallel incubation of slides in the presence of 1 μM atropine. Incubations were terminated by two consecutive 15-min washes with 25 mM ice-cold Tris buffer, followed by a quick dip in ice-cold distilled water to remove buffer salts. Slides were rapidly dried in a stream of cold air. Dried sections were juxtaposed tightly against glass coverslips that had been coated with Ilford K.5 emulsion (Ilford Scientific Products, Cheshire, UK). Slides were then stored in desiccated light-tight boxes at 4° until development after an exposure period of 3 months. Sections were stained with 1% cresyl fast violet and examined under a Zeiss microscope equipped with dark-field and bright-field illumination.

Results

Saturation experiments. Specific [³H]NMS binding to muscarinic receptors of rat heart and salivary glands was saturable and best described by the interaction of the radioligand with a single population of high affinity binding sites. The affinities (K_d) were 0.09 ± 0.02 and 0.35 ± 0.04 nM in rat salivary glands and heart, respectively. In rat cerebral cortex, [³H]telenzepine, at a concentration of 0.4 nM, labeled exclusively the M_1 receptors. [³H]Telenzepine/telenzepine displacement studies revealed a K_d value of 0.62 nM.

When [³H]Ba 679 BR and [³H]NMS were used to label muscarinic receptors in human lung membranes, specific binding of both radioligands was saturable (Figs. 2 and 3). Scatchard analysis of the saturation isotherms indicated that both radioligands bound to a homogeneous receptor population, with the affinities and receptor densities listed in Table 1.

Specific [³H]Ba 679 BR (0.6 nM) binding to cryostat sections of human lung reached steady state within 90–100 min of incubation at 30° and accounted for 80–90% of total binding (data not shown). The [³H]Ba 679 BR binding to human peripheral lung sections was saturable, and Scatchard analysis showed a single class of binding sites, with a maximum binding capacity of 54 ± 7 fmol/mg of protein and an equilibrium dissociation constant of 330 ± 130 pM (Fig. 4).

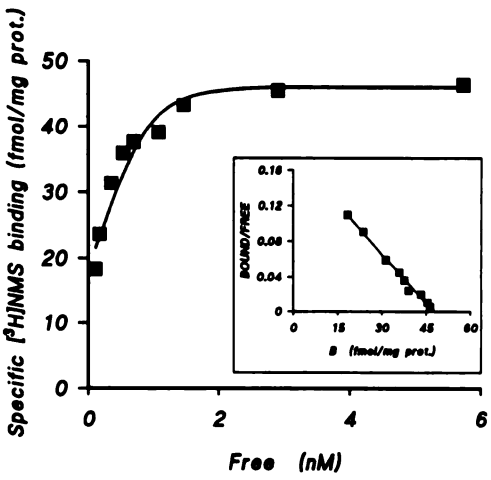

Fig. 2. Saturation of [³H]NMS binding sites in human lung membranes. *Inset*, Scatchard transformation of specific [³H]NMS saturation data. The data shown are the average of duplicate determinations at each *point* and are representative of three other similar experiments. The *curves* were drawn freehand.

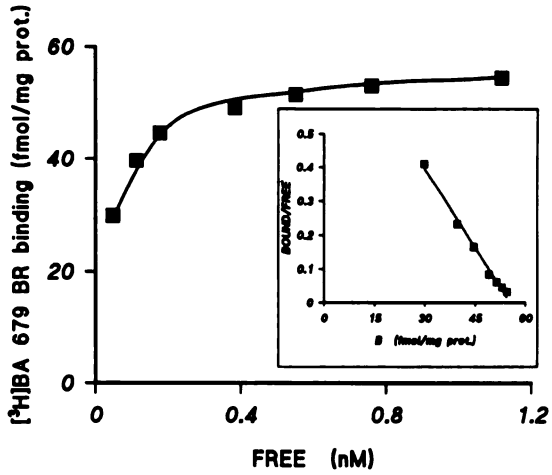

Fig. 3. Saturation of [³H]Ba 679 BR binding sites in human lung membranes. *Inset*, Scatchard transformation of specific [³H]Ba 679 BR saturation data. The data shown are the average of duplicate determinations at each *point* and are representative of three other similar experiments. The *curves* were drawn freehand.

TABLE 1

Binding characteristics of [³H]NMS and [³H]Ba 679 BR in human lung membranes

Receptor densities (B_{max}) and equilibrium dissociation constants (K_d) are means ± standard errors of four independent experiments performed in duplicate.

	K_d	B_{max}
	pM	fmol/mg of protein
[³H]NMS	184 ± 45	52 ± 6
[³H]Ba 679 BR	38.6 ± 9.7	48 ± 7

Competition experiments. In competition studies, Ba 679 BR and ipratropium bromide fully inhibited the specific binding of [³H]NMS (human lung, rat heart, and rat salivary glands) and [³H]telenzepine (cerebral cortex) in a concentration-de-

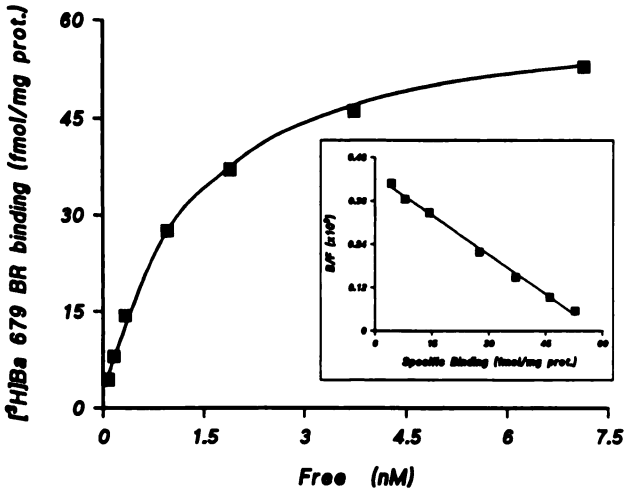

Fig. 4. Saturation of [^{3}H]Ba 679 BR binding sites in human lung sections. *Inset*, Scatchard transformation of specific [^{3}H]Ba 679 BR saturation data. The data shown are the average of triplicate determinations at each *point* and are representative of two other similar experiments. The *curves* were drawn freehand.

pendent manner (Figs. 5 and 6A). [^{3}H]NMS and [^{3}H]telenzepine labeled homogeneous binding sites that were not discriminated by the drugs used, inasmuch as both of the antagonists examined produced mass action competition curves compatible with the existence of a single receptor subtype in the different membrane preparations used. The results of the competition studies are shown in Table 2.

Selective muscarinic antagonists were also tested for their ability to compete with [^{3}H]Ba 679 BR (0.6 nM) for specific binding sites in human lung homogenates (Fig. 6B). The M_2-selective antagonist methoctramine displaced specific [^{3}H]Ba 679 BR binding according to the law of mass action, with steep slopes, giving a Hill coefficient not significantly different from unity. However, the M_1-selective antagonist pirenzepine and the M_1/M_3-selective antagonist 4-DAMP inhibited specific [^{3}H]Ba 679 BR binding with Hill coefficients significantly less than unity, as illustrated in Fig. 6B by the shallow displacement curves for both antagonists. Two-site analysis of the data resulted in a significant improvement of the fit, indicating the presence of a mixed population of receptors in human lung. Seventy-one to 74% of total [^{3}H]Ba 679 BR binding sites were recognized by pirenzepine and 4-DAMP with high affinity. The K_i values are summarized in Table 3.

Due to the extremely slow dissociation kinetics of [^{3}H]Ba 679 BR in human lung, equilibrium conditions with this radioligand might be difficult to achieve. The mathematical model described by Motulsky and Mahan (21) gives a guide to the time needed for a competition curve to reach equilibrium. Although the model is valid only when the radioligand and the competitor bind reversibly to a single class of receptors, following the law of mass action, the predicted time for a competitive binding experiment to reach equilibrium depends on the ligand with the slowest dissociation and is equal in our case to 5 times the [^{3}H]Ba 679 BR-receptor complex half-life (which is approximately 18 hr). This time may be even longer in the presence of a competitor. Experiments were carried out with an incubation period of 24 hr. Parallel control experiments were performed to ensure that this incubation period did not degrade the receptors (data not shown). Our results showed that a 24-hr incubation period gave virtually identical results, compared with the 3-hr incubation period (Table 3). The reason for this is that the predicted incubation time is halved in the presence of a high concentration of the radioligand (the ratio of the radioligand concentration to its K_d value was approximately equal to 15 in our experiment). Another plausible explanation is that the mathematical model described by Motulsky and Mahan (21) is not valid when the tissue expresses a mixture of receptors and the radioligand exhibits differences in binding kinetic parameters for these receptors, which is apparently the case in our study. Moreover, the profile of muscarinic receptor expression derived from these competition curves agrees with published data using a radioligand with faster dissociation kinetics (i.e., [^{3}H]quinuclidinyl benzilate, $k_{-1} = 4.6\ 10^{-3}\ min^{-1}$) (22).

Kinetic experiments. The dissociation of Ba 679 BR and ipratropium bromide from human lung membranes was estimated indirectly by measuring the rate of [^{3}H]NMS association after dilution to induce antagonist dissociation. These experiments showed a marked difference in the apparent dissociation profile between Ba 679 BR and ipratropium bromide (Fig. 7).

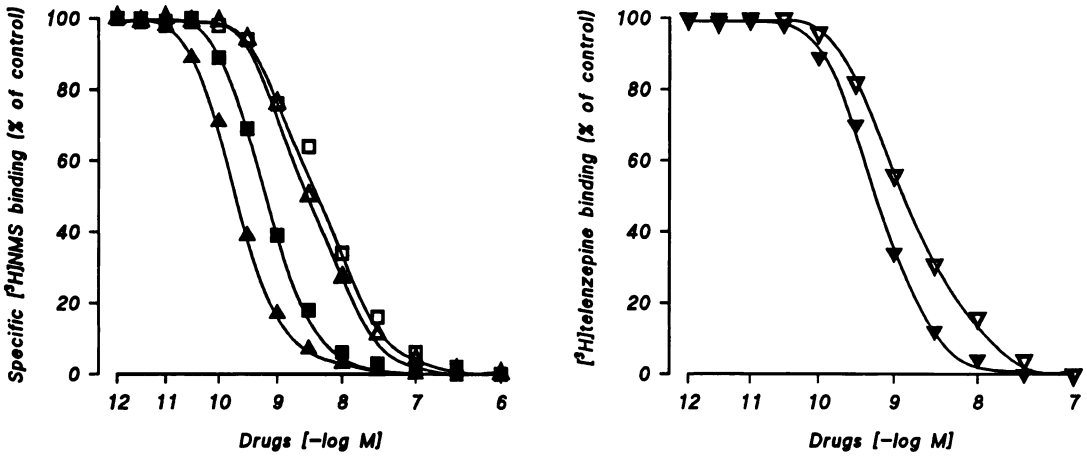

Fig. 5. Inhibition of [^{3}H]NMS and [^{3}H]telenzepine binding by Ba 679 BR (*closed symbols*) and ipratropium bromide (*open symbols*) in rat cerebral cortex (*inverted triangles*), heart (*squares*), and salivary glands (*triangles*). Values are means from three to six independent experiments performed in duplicate with separate membrane preparations. The *curves* were drawn freehand and do not represent the best fit.

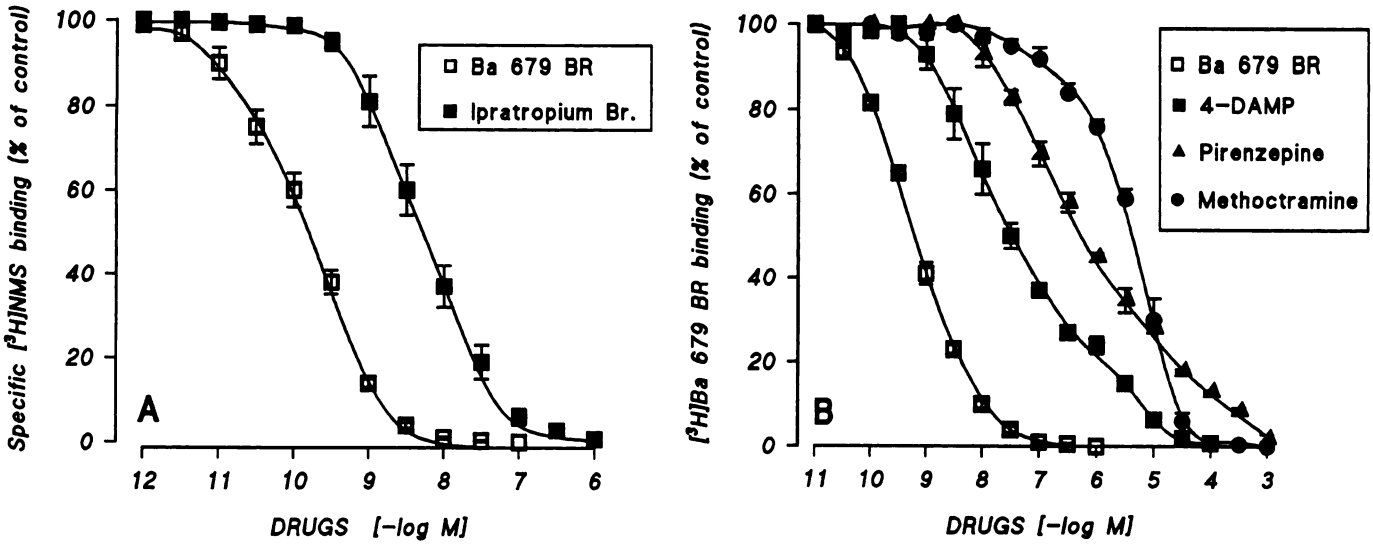

Fig. 6. Inhibition by selected muscarinic antagonists of [³H]NMS (A) and [³H]Ba 679 BR (B) binding in human lung membranes. Values are means ± standard errors from three to six independent experiments performed in duplicate with separate membrane preparations. The *curves* were drawn freehand and do not represent the best fit.

TABLE 2

Inhibition by Ba 679 BR and ipratropium bromide of [³H]telenzepine (rat cerebral cortex) and [³H]NMS (human lung and rat heart and salivary glands) bindings

Inhibitory dissociation constant (K_i) values and Hill coefficients (n_H) were determined from competitive binding curves (illustrated in Figs. 5 and 6A). Values are means ± standard errors of three to six independent experiments performed in duplicate with separate membrane preparations.

	Human lung	Cerebral cortex (M_1)	Heart (M_2)	Salivary glands (M_3)
Ba 679 BR				
K_i (nM)	0.026 ± 0.011	0.21 ± 0.05	0.22 ± 0.06	0.06 ± 0.02
n_H	0.97 ± 0.22	1.0 ± 0.06	1.03 ± 0.07	1.08 ± 0.12
Ipratropium bromide				
K_i (nM)	0.51 ± 0.11	1.24 ± 0.36	3.54 ± 1.27	0.64 ± 0.07
n_H	0.92 ± 0.02	0.92 ± 0.01	0.99 ± 0.04	1.01 ± 0.02

TABLE 3

Inhibition by selected muscarinic antagonists of [³H]Ba 679 BR binding to human peripheral lung membranes

Values are means ± of three to six independent experiments performed in duplicate with separate membrane preparations. Inhibitory dissociation constant (K_i) values were determined from competitive binding curves (illustrated in Fig. 6B for the 3-hr incubation period) with the computerized method LIGAND, as described by Munson and Rodbard (19). The n_H value is the slope of the curve (Hill coefficiednt), and the proportion of specifically [³H]Ba 679 BR-labeled binding sites that showed high or low affinity for each antagonist is shown.

	3-hr incubation			24-hr incubation		
	n_H	K_i	Proportion	n_H	K_i	Proportion
Ba 679 BR	0.86 ± 0.02	0.12 ± 0.02	100	0.98 ± 0.08	0.10 ± 0.01	100
Ipratropium	0.91 ± 0.04	1.12 ± 0.1	100	0.95 ± 0.02	1.31 ± 0.15	100
Pirenzepine	0.44 ± 0.02[a]	15.5 ± 3.1	71 ± 2	0.76 ± 0.04[a]	2.63 ± 0.52	74 ± 11
		6900 ± 2110	29 ± 2		518 ± 69	26 ± 11
Methoctramine	1.14 ± 0.03	314 ± 124	100	1.19 ± 0.06	149 ± 24	100
4-DAMP	0.48 ± 0.02[a]	0.86 ± 0.38	74 ± 4	0.74 ± 0.07[a]	1.29 ± 0.87	69 ± 14
		484 ± 170	26 ± 4		401 ± 124	31 ± 14

[a] Statistically significant difference from unity, using Student's *t* test.

Ipratropium bromide dissociated so rapidly ($t_{½}$ = 11.4 min) that there was little difference in the rate of [³H]NMS association, compared with vehicle-treated membranes, whereas Ba 679 BR had a marked protective effect (>70% inhibition) against [³H]NMS binding, which persisted for 90 min.

Using [³H]Ba 679 BR, it was possible to monitor its dissociation profile directly. [³H]Ba 679 BR binding to human lung membranes reached steady state within 30 min of incubation and was stable for up to 7.5 hr (Fig. 8). The association kinetic data could be fitted well by a monoexponential function with an apparent rate constant (k_{obs}) of 0.175 ± 0.02 min^{-1} ($t_{½}$ = 3.96 min). The calculated association rate constant (k_1) was 2.73 ± 0.05 × 10^8 min^{-1} M^{-1}. The dissociation rate for [³H]Ba 679 BR was determined after preincubation of the lung membranes with [³H]Ba 679 BR (0.63 nM) for 120 min, by the addition of atropine (10 μM) to prevent tracer rebinding. The dissociation data could be described by a simple exponential function with a rate constant (k_{-1}) of 3.29 ± 0.18 × 10^{-3} min^{-1}, corresponding to a half-life of the complex ($t_{½}$) of 212 ± 11 min (Fig. 9). The kinetically determined dissociation constant (k_{-1}/k_1) of 12.07 ± 0.81 pM was close to that calculated under equilibrium binding conditions (Table 1).

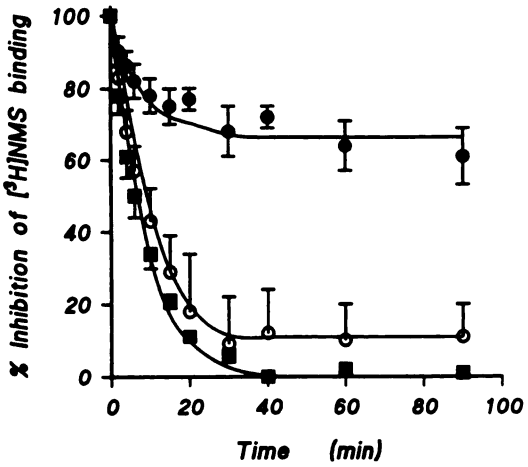

Fig. 7. [^{3}H]NMS binding to human lung muscarinic receptors occupied by Ba 679 BR (●) or ipratropium bromide (○). Human lung membranes were treated for 3 hr at 30° with assay buffer (■), Ba 679 BR (1 nM), or ipratropium bromide (100 nM). After this preincubation period, the volume of membrane suspension was then diluted 70-fold (to induce antagonist dissociation) with assay buffer containing a final [^{3}H]NMS concentration of 0.5 nM. The association of [^{3}H]NMS (expressed as percentage inhibition of [^{3}H]NMS binding, which reflects the percentage of Ba 679 BR- or ipratropium-occupied receptors) was measured at appropriate time intervals. Values are means ± standard errors from four independent experiments performed in triplicate with separate membrane preparations.

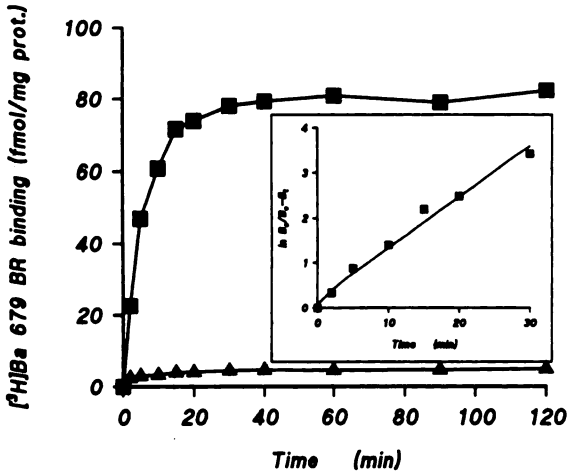

Fig. 8. Association kinetics of [^{3}H]Ba 679 BR binding to human lung membranes. Specific (■) and nonspecific (▲) [^{3}H]Ba 679 BR binding was measured at 30° after various time intervals. *Inset*, semilogarithmic plot of the association data. The data shown are the means of triplicate determinations at each *point* and are representative of three experiments. The *curves* were drawn freehand and do not represent the best fit.

Receptor autoradiography. Autoradiographic analysis showed specific labeling with [^{3}H]Ba 679 BR in human lung and trachea (Figs. 10 and 11). Autoradiograms of the human peripheral lung revealed that [^{3}H]Ba 679 BR binding sites were distributed with a dense and uniform labeling on alveolar walls (Fig. 10). The vascular smooth muscle and the endothelium were devoid of any specific labeling (data not shown). In human trachea, specific [^{3}H]Ba 679 BR binding sites were densely distributed on submucosal glands (Fig. 11), with no evidence of labeling over the epithelium or airway smooth muscle (data not shown).

In competition experiments, pirenzepine (100 nM) was as

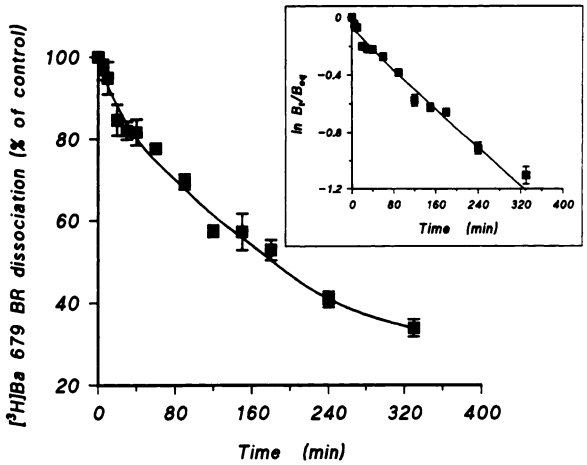

Fig. 9. Dissociation kinetics of [^{3}H]Ba 679 BR binding to human lung membranes. *Inset*, semilogarithmic plot of the dissociation data. The data shown are the means ± standard errors from three independent experiments performed in triplicate with separate membrane preparations. The *curves* were drawn freehand and do not represent the best fit.

effective as 4-DAMP (10 nM) in displacing [^{3}H]Ba 679 BR binding sites from alveolar walls and submucosal glands. However, methoctramine (100 nM) had no inhibitory effect on [^{3}H]Ba 679 BR binding sites in either tissue section (Figs. 10 and 11).

Discussion

Ba 679 BR is a new muscarinic antagonist developed as a bronchodilator for the treatment of patients with reversible obstruction airway disease. In this study, we have evaluated the affinity, the selectivity, and the distribution of Ba 679 BR binding sites in human lung membranes and tissue sections. The most important finding of this study is the very high affinity and the very slow dissociation profile of Ba 679 BR from human muscarinic receptors, which clearly distinguish it from the reference drug ipratropium bromide.

In saturation studies, [^{3}H]Ba 679 BR binds to a homogeneous population of muscarinic receptors in human lung membranes, with affinities in the subnanomolar concentration range. [^{3}H]Ba 679 BR labeled the same density of sites as did [^{3}H]NMS (Table 1). Receptor densities deduced from saturation experiments were slightly lower than those found by others (22–24), which may be due to the hydrophilic quaternary ammonium radioligands used ([^{3}H]Ba 679 BR and [^{3}H]NMS) (25), compared with [^{3}H]quinuclidinyl benzilate used in the previous studies (22–24). The affinity estimates of Ba 679 BR binding to human lung muscarinic receptors labeled with [^{3}H]NMS agree with those determined by direct labeling with [^{3}H]Ba 679 BR in either saturation or kinetic experiments (Table 1).

We have also investigated the selectivity of Ba 679 BR and ipratropium bromide in their interactions with rat cerebrocortical M_1 receptors labeled with [^{3}H]telenzepine and heart M_2 and salivary gland M_3 receptors labeled with [^{3}H]NMS. Ipratropium bromide bound to all of the receptor subtypes studied with almost the same high affinity, in agreement with published data (22). Similar to ipratropium bromide, Ba 679 BR showed no selectivity in its binding to M_1-M_3 receptors, although a 3.5-fold higher affinity at M_3 receptors, compared with M_1 and M_2 receptors, was observed. The dissociation constants of Ba 679

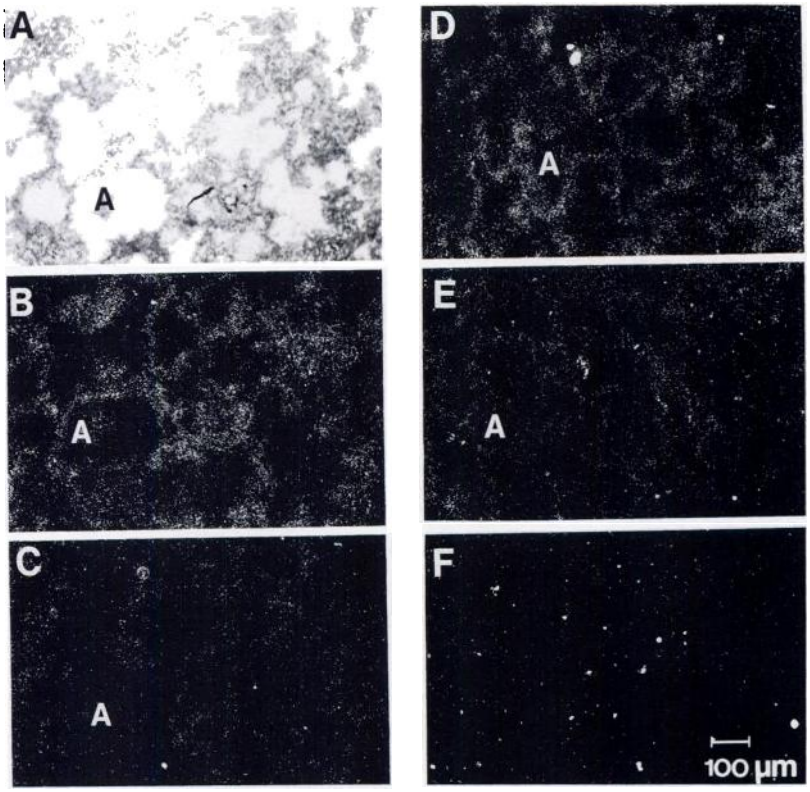

Fig. 10. Autoradiographic distribution of [^{3}H]Ba 679 BR binding sites in human peripheral lung. A, Bright-field photomicrograph stained with 1% cresyl fast violet, in which alveolar walls (*A*) are shown. B-F, Dark-field photomicrographs of adjacent sections, showing the distribution of autoradiographic grains after incubation with [^{3}H]Ba 679 BR (0.6 nM) alone (B) or in the presence of the M_1-selective antagonist pirenzepine (C), the M_2-selective antagonist methoctramine (D), the M_1/M_3-selective antagonist 4-DAMP (E), and the nonselective antagonist atropine (F). Binding sites were distributed on alveolar walls and were almost completely displaced by pirenzepine (100 nM) and 4-DAMP (10 nM) but not by methoctramine (100 nM).

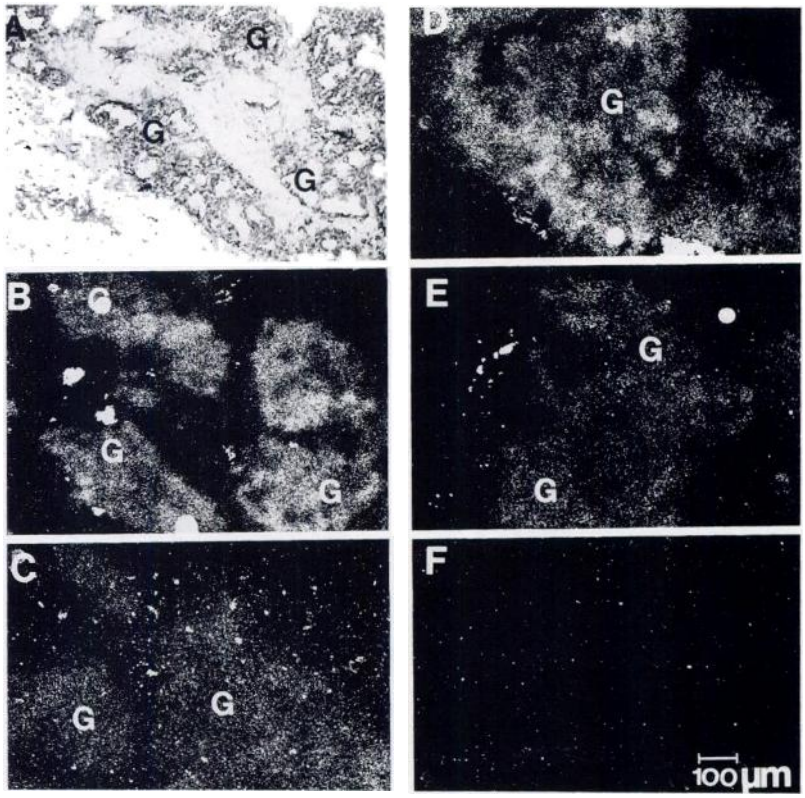

Fig. 11. Autoradiographic distribution of [^{3}H]Ba 679 BR binding sites in human trachea. A, Bright-field photomicrograph stained with 1% cresyl fast violet, in which submucosal glands (*G*) are shown. B-F, Dark-field photomicrographs of adjacent sections, showing the distribution of autoradiographic grains after incubation with [^{3}H]Ba 679 BR (0.6 nM) alone (B) or in the presence of the M_1-selective antagonist pirenzepine (C), the M_2-selective antagonist methoctramine (D), the M_1/M_3-selective antagonist 4-DAMP (E), and the nonselective antagonist atropine (F). Binding sites were distributed on submucosal glands and were partially displaced by pirenzepine (100 nM) and 4-DAMP (10 nM) but not by methoctramine (100 nM).

BR obtained at M_1-M_3 receptors are comparable to those determined using Chinese hamster ovary cells transfected with the human m1-m3 receptor genes (17). Compared with ipratropium bromide, Ba 679 BR displayed 10–20-fold higher affinity in its binding to human lung muscarinic receptors and 6–16-fold higher affinity for M_1 and M_2 receptors. It should be noted that the affinities of Ba 679 BR and ipratropium bromide for human lung muscarinic receptors were somewhat higher (2–5 times) when [^{3}H]NMS rather than [^{3}H]Ba 679 BR was used to label these sites.

Inhibition curves for the binding of three selective muscarinic antagonists to human lung muscarinic receptors labeled with

[^{3}H]Ba 679 BR are shown in Fig. 6B, and the calculated dissociation constants are listed in Table 3. Due to the extremely slow dissociation kinetics of [^{3}H]Ba 679 BR in human lung, competition experiments were performed with 3-hr (Fig. 6B) and 24-hr incubation periods. The results indicate that the longer incubation period gives results virtually identical to those obtained with the relatively short incubation period (Table 3). The displacement curves for the M_2-selective antagonist methoctramine could be best described by interaction with a single population of receptors, in agreement with our previous findings (24). The lack of a high affinity binding site for methoctramine suggests an absence of muscarinic M_2 receptors. Indeed, the affinity of methoctramine for human lung muscarinic receptors (K_i values of 149–314 nM) is similar to values reported for interactions with M_1 and/or M_3 receptors (26–28). In agreement with previous studies (22–24), pirenzepine competition experiments generated shallow curves that could be described by a two-binding site model. The affinity of 2.63–15.5 nM for 71–74% of the sites agrees well with the affinity of pirenzepine for M_1 receptors (3, 29). This finding has recently been substantiated by the detection in human lung of mRNA encoding m1 receptors (30). Heterogeneity of human lung muscarinic receptors was also revealed by competitive experiments with 4-DAMP. This antagonist recognized 69–74% of total [^{3}H]Ba 679 BR binding sites with high affinity. The high affinity binding constant was close to the M_1 and/or M_3 receptor affinity estimates for 4-DAMP (2, 14). Although the low affinity pirenzepine and 4-DAMP binding sites are indicative of M_2 receptor labeling, the methoctramine/[^{3}H]Ba 679 BR competition curves argue against the presence of a significant population of these receptors in human lung. In an attempt to address this question, we performed direct labeling of human lung M_2 muscarinic receptors with the M_2-selective antagonist [^{3}H]AF-DX 384 (data not shown). Unfortunately, the high level of nonspecific binding precluded any further quantification and characterization of the [^{3}H]AF-DX 384 binding sites in human lung. The reason for the apparent discrepancy regarding the presence of M_2 receptors in human lung is unclear and might be due to difficulty in discriminating between two types of sites with radioligand binding methods when one of the sites is low in abundance or when the ratio of dissociation constants of the selective ligand for the two sites is small (31). Previous studies in our laboratory have demonstrated the presence of mRNA for m1 receptors but an absence of m2 receptor mRNA in human lung (30).

In functional studies, Ba 679 BR antagonized the contraction of guinea pig trachea with high affinity ($pA_2 = 9.51$) and showed a very long duration of action (17). We have investigated the dissociation profile of Ba 679 BR from human lung muscarinic receptors as a potential mechanism whereby this drug achieves its duration of action. We designed experiments to study the dissociation of Ba 679 BR and ipratropium bromide from human lung muscarinic receptors by monitoring the rate of [^{3}H]NMS association (Fig. 7). Human lung membranes were preincubated for 3 hr with Ba 679 BR (1 nM) or ipratropium bromide (100 nM), to occupy 80–90% of the receptors. To induce antagonist dissociation, the volume of the membrane suspension was then increased 70-fold with assay buffer containing [^{3}H]NMS, thereby reducing the concentration of both antagonists. The time course of [^{3}H]NMS association in buffer- and ipratropium-pretreated membranes was rapid and reached equilibrium within 30–40 min of incubation ($t_{1/2}$ = 11.4 min). In Ba 679 BR-pretreated membranes, the rate of [^{3}H]NMS association (shown in Fig. 7 as the percentage of Ba 679 BR-occupied receptors) was considerably slower. This result suggests that [^{3}H]NMS binding to human lung muscarinic receptors was probably limited by the slow dissociation rate of Ba 679 BR.

By using direct labeling of human lung muscarinic receptors with [^{3}H]Ba 679 BR, we were able to confirm the slow dissociation profile of this compound. Fig. 9 shows that the dissociation of [^{3}H]Ba 679 BR from lung membranes is best described by a simple exponential function with a rate constant (k_{-1}) of $3.29 \pm 0.18 \times 10^{-3}$ min^{-1}. The calculated half-life of the complex was 212 ± 11 min.

Prolonged inhibitory effects by Ba 679 BR have been observed in functional tests. In patients with chronic obstructive pulmonary disease, inhalation of Ba 679 BR (10–40 μg) results in a significant bronchodilatation that persists for >10 hr (32). In anesthetized dogs, inhaled Ba 679 BR at 1 g/liter provided 90–100% protection against acetylcholine-induced bronchoconstriction that lasted for >360 min. At the same dose, the bronchoprotective effect of ipratropium bromide is modest and declines to nearly 20% after 90 min (17). Comparable results have been obtained in rabbits and guinea pigs *in vivo* (33). Thus, there seems to be a close correlation between the binding experiments obtained in human lung and the functional data regarding the dissociation half-lives of the antagonists.

Despite its nonselectivity in equilibrium binding studies, Ba 679 BR has been proposed as a "kinetic receptor subtype-selective drug" (17). In Chinese hamster ovary cells expressing the human m1, m2, and m3 muscarinic receptor genes, [^{3}H]Ba 679 BR dissociates faster from human m2 receptors ($t_{1/2}$ = 3.6 hr) than from m1 ($t_{1/2}$ = 14.6 hr) or m3 ($t_{1/2}$ = 34.7 hr) receptors. We, and others (22–24), have shown that human peripheral lung expresses a majority of muscarinic receptors of the M_1 receptor subtype. However, the dissociation half-life of 212 min for the [^{3}H]Ba 679 BR-human lung muscarinic receptor complex is not in agreement with that obtained with either human m1 or m3 receptors. Moreover, there is no evidence for a biphasic profile of [^{3}H]Ba 679 BR dissociation from human lung receptors over the time points investigated. The reason for this discrepancy could be due to differences in tissues (i.e., transfected cell lines versus whole tissue) and/or in the binding assay conditions (i.e., 23° versus 30°) (34).

To determine the tissue distribution of [^{3}H]Ba 679 BR, autoradiographic mapping has been performed in human lung and airways. Binding experiments with cryostat sections of peripheral lung revealed the existence of a single class of saturable and high affinity [^{3}H]Ba 679 BR binding sites. The B_{max} value determined in lung sections is close to that obtained in lung homogenates and agrees with published data (35). However, the affinity of [^{3}H]Ba 679 BR derived from lung sections was slightly lower (8.5-fold) than that determined for lung homogenates, which might reflect differences in experimental procedures.

Autoradiograms indicated that [^{3}H]Ba 679 BR binding sites are densely distributed on alveolar walls and submucosal glands (Figs. 10 and 11). There is no evidence of significant labeling over airway epithelium, blood vessels, or airway smooth muscle. In human peripheral lung, M_1 receptors are present on alveolar walls, inasmuch as [^{3}H]Ba 679 BR binding was almost com-

pletely inhibited by the M_1-selective antagonist pirenzepine and by the M_1/M_3-selective antagonist 4-DAMP, which is in agreement with the binding data obtained in homogenates from this tissue. Furthermore, these sites have been previously shown to be selectively labeled by [^{3}H]pirenzepine (35), and m1 mRNA has been detected in this location (30). The specific binding of [^{3}H]Ba 679 BR to tracheal submucosal glands was partially displaced by pirenzepine and 4-DAMP, suggesting the presence of both M_1 and M_3 receptors, which is in agreement with other autoradiographic data obtained in human intrapulmonary bronchi (35). The presence of M_3 receptors in submucosal glands is consistent with the detection of m3 mRNA in these cells (30). In human lung and trachea, methoctramine had no inhibitory effect on the specific [^{3}H]Ba 679 BR binding sites, suggesting the lack of M_2 receptors in both types of tissue sections.

In human trachea as well as segmental bronchus, we were unable to detect any [^{3}H]Ba 679 BR binding sites on airway smooth muscle, which disagrees with the findings of Van Koppen *et al.* (36) and our previous autoradiographic study in human lung (35). The failure of [^{3}H]Ba 679 BR to label these sites may be due to the low density of muscarinic receptors in airway smooth muscle (35, 36).

In conclusion, we have shown that Ba 679 BR (i) binds human lung muscarinic receptors with very high affinity, (ii) is at least 10 times more potent than ipratropium bromide, (iii) displays a very slow dissociation profile, and (iv) has binding sites that are densely distributed on alveolar walls and submucosal glands. Furthermore, we suggest that the slow dissociation profile of Ba 679 BR might be the underlying mechanism by which this drug achieves its duration of action and therefore represents an improvement over conventional anticholinergic approaches for the treatment of obstructive airway disease.

Acknowledgments

We thank Mr. P. Seldon for printing photographs.

References

1. Mitchelson, F. Muscarinic receptor differentiation. *Pharmacol. Ther.* **37**:357–423 (1988).
2. Waelbroeck, M., M. Tastenoy, J. Camus, and J. Christophe. Binding of selective antagonists to four muscarinic receptors (M_1 to M_4) in rat forebrain. *Mol. Pharmacol.* **38**:267–273 (1990).
3. Dörje, F., J. Wess, G. Lambrecht, R. Tacke, E. Mutschler, and M. R. Brann. Antagonist binding profiles of five cloned human muscarinic receptor subtypes. *J. Pharmacol. Exp. Ther.* **256**:727–733 (1991).
4. Hulme, E. C., N. J. M. Birdsall, and N. J. Buckley. Muscarinic receptor subtypes. *Annu. Rev. Pharmacol. Toxicol.* **30**:633–673 (1990).
5. Akiba, I., T. Kubo, A. Maeda, H. Bujo, J. Nakai, M. Mishina, and S. Numa. Primary structure of porcine muscarinic acetylcholine receptor III and antagonist binding studies. *FEBS Lett.* **235**:257–261 (1988).
6. Brann, M. R., N. J. Buckley, and T. I. Bonner. The striatum and cerebral cortex express different muscarinic receptor mRNAs. *FEBS Lett.* **230**:90–94 (1988).
7. Buckley, N. J., T. I. Bonner, C. M. Buckley, and M. R. Brann. Antagonist binding properties of five cloned muscarinic receptors expressed in CHO-K1 cells. *Mol. Pharmacol.* **35**:469–476 (1989).
8. Vilaro, M. T., J. M. Palacios, and G. Mengod. Localization of m5 muscarinic receptor mRNA in rat brain examined by *in situ* hybridization histochemistry. *Neurosci. Lett.* **114**:154–159 (1990).
9. Barnes, P. J. Muscarinic receptors in airways: recent developments. *J. Appl. Physiol.* **68**:1777–1785 (1990).
10. Barnes, P. J. Muscarinic receptor subtypes in airways. *Life Sci.* **52**:521–528 (1993).
11. Lammers, J.-W., P. Minette, M. McCusker, and P. J. Barnes. The role of pirenzepine-sensitive (M_1) muscarinic receptors in vagally mediated bronchoconstriction in humans. *Am. Rev. Respir. Dis.* **139**:446–449 (1989).
12. Minette, P., and P. J. Barnes. Prejunctional inhibitory muscarinic receptors on cholinergic nerves in human and guinea pig airways. *J. Appl. Physiol.* **64**:2532–2537 (1988).
13. Haddad, E.-B., Y. Landry, and J.-P. Gies. Muscarinic receptor subtypes in guinea pig airways. *Am. J. Physiol.* **261**:L327–L333 (1991).
14. Lazareno, S., N. J. Buckley, and F. F. Roberts. Characterization of muscarinic M_4 binding sites in rabbit lung, chicken heart and NG108–15 cells. *Mol. Pharmacol.* **38**:805–815 (1990).
15. Dörje, F., A. I. Levey, and M. R. Brann. Immunological detection of muscarinic receptor subtype proteins (m1-m5) in rabbit peripheral tissues. *Mol. Pharmacol.* **40**:459–462 (1991).
16. Gross, N. J. Anticholinergic agents in the treatment of chronic bronchitis and emphysema, in *Chronic Obstructive Pulmonary Disease* (N. S. Cherniack, ed.). W. B. Saunders, Philadelphia, 490–494 (1991).
17. Disse, B., R. Reichel, G. Speck, W. Traunecker, K. L. Rominger, and R. Hammer. Ba 679 BR, a novel long-acting anticholinergic bronchodilator. *Life Sci.* **52**:537–544 (1993).
18. Lowry, O. H., N. J. Rosebrough, A. L. Farr, and R. J. Randall. Protein measurement with the Folin phenol reagent. *J. Biol. Chem.* **193**:265–275 (1951).
19. Munson, J., and D. Rodbard. LIGAND: a versatile computerized approach to characterization of ligand-binding systems. *Anal. Biochem.* **107**:220–239 (1980).
20. Haddad, E.-B., Y. Landry, and J.-P. Gies. Sialic acid residues as catalyst for M_2-muscarinic agonist-receptor interactions. *Mol. Pharmacol.* **37**:682–688 (1990).
21. Motulsky, H. J., and L. C. Mahan. The kinetics of competitive radioligand binding predicted by the law of mass action. *Mol. Pharmacol.* **25**:1–9 (1984).
22. Bloom, J. W., M. Halonen, and H. I. Yamamura. Characterization of muscarinic cholinergic receptor subtypes in human peripheral lung. *J. Pharmacol. Exp. Ther.* **244**:625–632 (1988).
23. Gies, J.-P., C. Bertrand, P. Venderheyden, F. Waeldele, P. Dumont, G. Pauli, and Y. Landry. Characterization of muscarinic receptors in human, guinea pig and rat lung. *J. Pharmacol. Exp. Ther.* **250**:309–315 (1989).
24. Mak, J. C. W., and P. J. Barnes. Muscarinic receptor subtypes in human and guinea pig lung. *Eur. J. Pharmacol.* **164**:223–230 (1989).
25. Lee, J.-H., and E. E. El-Fakahany. Heterogeneity of binding of muscarinic receptor antagonists in rat brain homogenates. *J. Pharmacol. Exp. Ther.* **233**:707–714 (1985).
26. Giraldo, E., R. Micheletti, E. Montagna, A. Giachetti, M. A. Viganò, H. Ladinsky, and C. Melchiorre. Binding and functional characterization of the cardioselective muscarinic antagonist methoctramine. *J. Pharmacol. Exp. Ther.* **244**:1016–1020 (1988).
27. Lazareno, S., and F. F. Roberts. Functional and binding studies with muscarinic M_2-subtype selective antagonists. *Br. J. Pharmacol.* **98**:309–317 (1989).
28. Michel, A. D., and R. L. Whiting. Methoctramine reveals heterogeneity of M_2 muscarinic receptors in longitudinal ileal smooth muscle membranes. *Eur. J. Pharmacol.* **145**:305–311 (1988).
29. Kromer, W., E. Baron, M. Beinborn, R. Boer, and M. Eltze. Characterization of the muscarine receptor type on paracrine cells activated by McN-A-343 in the mouse isolated stomach. *Naunyn-Schmiedebergs Arch. Pharmacol.* **341**:165–170 (1990).
30. Mak, J. C. W., J. N. Baraniuk, and P. J. Barnes. Localization of muscarinic receptor subtype mRNAs in human lung. *Am. J. Respir. Cell. Mol. Biol.* **7**:344–348 (1992).
31. De Lean, A., A. A. Hancock, and R. J. Lefkowitz. Validation and statistical analysis of a computer modeling method for quantitative analysis of radioligand binding data for mixtures of pharmacological receptor subtypes. *Mol. Pharmacol.* **21**:5–16 (1981).
32. Maesen, F. P. V., J. J. Smeets, M. A. L. Costongs, F. D. M. Wald, and P. J. G. Cornelissen. Ba 679 BR, a new long-acting antimuscarinic bronchodilator: a pilot dose escalator study in COPD. *Eur. Respir. J.* **6**:1031–1036 (1993).
33. Reichel, R., and W. Traunecker. Pharmacological profile of Ba 679 BR, a new long acting anticholinergic bronchodilator. *Naunyn-Schmiedebergs Arch. Pharmacol.* **347**:R112 (1993).
34. Pedder, E. K., P. Eveleigh, D. Poyner, E. C. Hulme, and N. J. M. Birdsall. Modulation of the structure-binding relationships of antagonists for muscarinic acetylcholine receptor subtypes. *Br. J. Pharmacol.* **103**:1561–1567 (1991).
35. Mak, J. C. W., and P. J. Barnes. Autoradiographic visualization of muscarinic receptor subtypes in human and guinea pig lung. *Am. Rev. Respir. Dis.* **141**:1559–1568 (1990).
36. Van Koppen, C. J., W. M. Blankesteijn, A. B. M. Klaassen, J. F. R. De Miranda, A. J. Beld, and A. M. Van Ginneken. Autoradiographic visualization of muscarinic receptors in human bronchi. *J. Pharmacol. Exp. Ther.* **244**:760–764 (1988).

Send reprint requests to: Peter J. Barnes, Department of Thoracic Medicine, National Heart and Lung Institute, Dovehouse Street, London SW3 6LY, UK.